PHILOSOPHICAL TRANSACTIONS OF THE ROYAL SOCIETY A

Phil. Trans. R. Soc. A (2006) **364**, 2309–2334
doi:10.1098/rsta.2006.1827
Published online 27 July 2006

Delayed feedback control of chaos

By Kestutis Pyragas*

T&T Semiconductor Physics Institute, 11 A. Goštauto, 011088 Vilnius, Lithuania

Time-delayed feedback control is well known as a practical method for stabilizing unstable periodic orbits embedded in chaotic attractors. The method is based on applying feedback perturbation proportional to the deviation of the current state of the system from its state one period in the past, so that the control signal vanishes when the stabilization of the target orbit is attained. A brief review on experimental implementations, applications for theoretical models and most important modifications of the method is presented. Recent advancements in the theory, as well as an idea of using an unstable degree of freedom in a feedback loop to avoid a well-known topological limitation of the method, are described in detail.

Keywords: dynamical system; controlling chaos; delayed feedback; time-delay autosynchronization; Pyragas method; unstable periodic orbit

1. Introduction

Control theory is one of the central subjects in engineering science. Despite the fact that engineers and applied mathematicians have been dealing with control problems for a long time, an idea of controlling chaos has been introduced relatively recently (Ott *et al.* 1990). This new idea has attracted great interest among physicists and boosted an enormous amount of work on control problems. Why are chaotic systems interesting subjects for control theory and applications? The major ingredient for the control of chaos is the observation that a chaotic set, on which the trajectory of the chaotic process lives, has embedded within it a large number of unstable periodic orbits (UPOs). In addition, owing to ergodicity, the trajectory visits or accesses the neighbourhood of each of these periodic orbits. Some of these periodic orbits may correspond to a desired system's performance according to some criterion. The second ingredient is the realization that chaos, while signifying sensitive dependence on small changes to the current state and henceforth rendering the system state unpredictable in the long term, also implies that the system's behaviour can be altered by using small perturbations. Then, the accessibility of the chaotic system to many different periodic orbits, combined with its sensitivity to small perturbations, allows for the control and the manipulation of the chaotic process. These ideas stimulated

*pyragas@pfi.lt

One contribution of 15 to a Theme Issue 'Exploiting chaotic properties of dynamical systems for their control'.

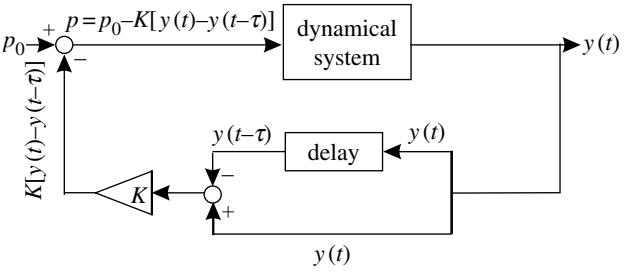

Figure 1. Block diagram of the delayed feedback control method. $y(t)$, is an output variable; p, a control parameter; p_0, its value at which the dynamical system has an unstable periodic orbit with a period τ; and K, the feedback gain.

the development of a rich variety of new chaos-control techniques (see Shinbrot *et al.* 1993; Kapitaniak 1996; Shuster 1999; Chen & Raton 2000; Boccaletti *et al.* 2000; Chen & Yu 2003 for review), among which the delayed feedback control (DFC) method proposed by Pyragas (1992) has gained widespread acceptance.

The DFC method is reference-free and makes use of a control signal obtained from the difference between the current state of the system and the state of the system delayed by one period of the UPO. The block diagram of the method is presented in figure 1. Alternatively, the DFC method is referred to as a method of time-delay autosynchronization, since the stabilization of the target orbit manifests itself as a synchronization of the current state of the system with its delayed state. The method allows us to treat the controlled system as a black box; no exact knowledge of either the form of the periodic orbit or the system of equations is needed. Taking into account only the period of the unstable orbit, the system under control automatically settles on the target periodic motion, and the stability of this motion is maintained with only small perturbations. The DFC algorithm is especially superior for fast dynamical systems, since it does not require any real-time computer processing. Experimental implementations, applications for theoretical models and most important modifications of the DFC method are briefly listed in §1*a–c*.

(*a*) *Experimental implementations*

The time-delayed feedback control has been successfully used in experimental contexts, which are quite diverse. Pyragas & Tamaševičius (1993), Kittel *et al.* (1994), Gauthier *et al.* (1994) and Celka (1994) verified it for electronic chaos oscillators. Hikihara & Kawagoshi (1996) and Christini *et al.* (1997) stabilized UPOs in mechanical pendulums. Bielawski *et al.* (1994), Basso *et al.* (1997*a*,*b*) and Lu *et al.* (1998) applied the DFC to laser systems. Pierre *et al.* (1996) investigated the DFC to a gas discharge system, Mausbach *et al.* (1997) stabilized ionization wave chaos, Fukuyama *et al.* (2002) controlled chaos caused by the current-driven ion acoustic instability and Gravier *et al.* (2000) stabilized drift waves in a magnetized laboratory plasma. An application of the DFC to a hydrodynamic system, namely, a chaotic Taylor–Couette flow, was considered by Lüthje *et al.* (2001). Parmananda *et al.* (1999) and Guderian *et al.* (1998) used the DFC to control electrochemical systems. Benner & Just (2002)

stabilized a UPO in a high-power ferromagnetic resonance system. A possibility of using the DFC to control helicopter rotor blades was considered by Krodkiewski & Faragher (2000). Sugimoto & Osuka (2002) applied the DFC to walking control of a robot. Lastly, Hall *et al.* (1997) used the DFC for a cardiac system.

(*b*) *Applications for theoretical models*

The DFC method has been verified for a large number of theoretical models from different fields. Simmendinger & Hess (1996) proposed an all-optical scheme, based on the DFC, for controlling delay-induced chaotic behaviour of high-speed semiconductor lasers. The problem of stabilizing semiconductor laser arrays was considered by Munkel *et al.* (1997) and Simmendinger *et al.* (1999). Rappel *et al.* (1999) used the DFC for stabilization of spiral waves in an excitable media as a model of cardiac tissue in order to prevent the spiral wave break-up. Konishi *et al.* (1999) applied the DFC to a model of a car following traffic. Batlle *et al.* (1999) implemented the DFC in a model of a buck converter. Bleich & Socolar (2000) showed that the DFC can stabilize regular behaviour in a paced, excitable oscillator described by the Fitzhugh–Nagumo equations. Holyst & Urbanowicz (2000) and Holyst *et al.* (2001) used the DFC to control chaos in the economical model. Tsui & Jones (2000) investigated the problem of chaotic satellite attitude control. The problem of controlling chaotic solitons by a time-delayed feedback mechanism was considered by Fronczak & Holyst (2002). Mensour & Longtin (1995) proposed the DFC as a method to store information in delay differential equations. Galvanetto (2002) demonstrated the DFC of chaotic systems with dry friction. Mitsubori & Aihara (2002) proposed a rather exotic application of the DFC, namely the control of chaotic roll motion of a flooded ship in waves. Recently, Rosenblum & Pikovsky (2004*a*,*b*) considered the influence of the DFC on the synchronization in an ensemble of globally coupled oscillators and discussed a possibility of using this approach to suppression of pathological brain rhythms.

(*c*) *Modifications*

A rich variety of modifications of the DFC has been suggested in order to improve its performance. Adaptive versions of the DFC with automatic adjustment of delay time (Kittel *et al.* 1995; Nakajima *et al.* 1997; Herrmann 2001) and control gain (Boccaletti & Arecchi 1995; Boccaletti *et al.* 1997) were considered. Basso *et al.* (1997*a*,*b*, 1998) showed that for a Lur'e system (system represented as a feedback connection between a linear dynamical part and a static nonlinearity), the DFC can be optimized by introducing a linear filter, with an appropriate transfer function, into a feedback loop. For spatially extended systems, various modifications based on spatially filtered signals were considered (Bleich *et al.* 1997; Hochheiser *et al.* 1997; Baba *et al.* 2002). The wave character of dynamics in some systems allows a simplification of the DFC algorithm by replacing the delay line with the spatially-distributed detectors. Mausbach *et al.* (1997) reported such a simplification for an ionization wave experiment in a conventional cold cathode-glow discharge tube. Owing to dispersion relations, the delay in time is equivalent to the spatial

displacement and the control signal can be constructed without using the delay line. Socolar *et al.* (1994) improved an original DFC scheme by using information from many previous states of the system. This extended delayed feedback control (EDFC) scheme achieves the stabilization of UPOs with a greater degree of instability (Pyragas 1995; Bleich & Socolar 1996). The EDFC presumably is the most important modification of the DFC and it will be discussed in detail in this paper.

The theory of the DFC is rather intricate, since it involves nonlinear delay differential equations. Even though linear stability analysis of the delayed feedback systems is difficult, some general analytical results have been obtained by Ushio (1996), Just *et al.* (1997), Nakajima (1997) and Nakajima & Ueda (1998*a*). It has been shown that the DFC can stabilize only a certain class of periodic orbits characterized by a finite torsion. More precisely, the limitation is that any UPO with an odd number of real Floquet multipliers (FMs) greater than unity (or with an odd number of real-positive Floquet exponents (FEs)) can never be stabilized by the DFC. This statement was first proved by Ushio (1996) for discrete-time systems. Just *et al.* (1997) and Nakajima (1997) proved the same limitation for the continuous-time DFC, and this proof was then extended for a wider class of delayed feedback schemes, including the EDFC (Nakajima & Ueda 1998*a*). Hence, it seems hard to overcome this inherent limitation. Two efforts, based on an oscillating feedback (Bielawski *et al.* 1993) and a half-period delay (Nakajima & Ueda 1998*b*), have been taken to obviate this drawback. In both these cases, the mechanism of stabilization is rather unclear. Besides, the method of Nakajima & Ueda (1998*b*) is valid only for a special case of symmetric orbits. The limitation has been recently eliminated in a new modification of the DFC that does not use the symmetry of UPOs (Pyragas 2001; Pyragas *et al.* 2004*b*). The key idea is to introduce into a feedback loop, an additional unstable degree of freedom that changes the total number of unstable torsion-free modes to an even number. Then, the idea of using unstable degrees of freedom in a feedback loop was drawn on to construct a simple adaptive controller for stabilizing unknown steady states of dynamical systems (Pyragas *et al.* 2002, 2004*a*).

Some recent theoretical results on the DFC method and the unstable controller are presented in more detail in the rest of the paper. §2 is devoted to the theory of the DFC. We show that the main stability properties of the system, controlled by time-delayed feedback, can be simply derived from a leading FE defining the system behaviour under proportional feedback control (PFC). We consider the EDFC versus the PFC and derive the transcendental equation relating the Floquet spectra of these two control methods. First, we suppose that the FE for the PFC depends linearly on the control gain and derives the main stability properties of the EDFC. Then, the case of nonlinear dependence is considered for the specific examples of the Rössler systems. For this example, we discuss the problem of optimizing the parameters of the delayed feedback controller. In §3, the problem of stabilizing torsion-free periodic orbits is considered. We start with a simple discrete time model and show that an unstable degree of freedom, introduced into a feedback loop, can overcome the limitation of the DFC method. Then, we propose a generalized modification of the DFC for torsion-free UPOs and demonstrate its efficiency for the Lorenz system. The paper concludes with §4.

2. Theory of delayed feedback control

If the equations governing the system dynamics are known, the success of the DFC method can be predicted by a linear stability analysis of the target orbit. Unfortunately, usual procedures for evaluating the FEs of such systems are rather intricate. Here, we show that the main stability properties of the system, controlled by time-delayed feedback, can be simply derived from a leading FE defining the system behaviour under PFC (Pyragas 2002). As a result, the optimal parameters of the delayed feedback controller can be evaluated without an explicit integration of delay differential equations.

Several numerical methods for the linear stability analysis of time-delayed feedback systems have been developed. The main difficulty of this analysis is related to the fact that periodic solutions of such systems have an infinite number of FEs, though only several FEs with the largest real parts are relevant for stability properties. The most straightforward method for evaluating several large FEs is described by Pyragas (1995). It adapts the usual procedure of estimating the Lyapunov exponents of strange attractors (Benettin *et al.* 1979), which requires a numerical integration of the variational system of delay differential equations. Bleich & Socolar (1996) devised an elegant method to obtain the stability domain of the system under EDFC, in which the delay terms in variational equations are eliminated owing to the Floquet theorem and the explicit integration of time-delay equations is avoided. Unfortunately, this method does not define the values of the FEs inside the stability domain and is unsuitable for optimization problems.

An approximate analytical method for estimating the FEs of time-delayed feedback systems has been developed by Just *et al.* (1997, 1999). Here, as well as in the paper by Bleich & Socolar (1996), the delay terms in variational equations are eliminated and the Floquet problem is reduced to the system of ordinary differential equations. However, the FEs of the reduced system depend on a parameter that is a function of the unknown FEs themselves. Just *et al.* (1997, 1999) solved the problem on the assumption that the FE of the reduced system depends linearly on the parameter. This method gives a better insight into the mechanism of DFC and leads to reasonable qualitative results. Here, we use a similar approach, but do not employ the above linear approximation and show how to obtain the exact results. In this section, we restrict ourselves to the UPOs that originated from a flip bifurcation.

(*a*) *Proportional versus delayed feedback*

Consider a dynamical system described by an ordinary differential equation

$$\dot{\boldsymbol{x}} = \boldsymbol{f}(\boldsymbol{x}, p, t), \tag{2.1}$$

where the vector $\boldsymbol{x} \in R^m$ defines the dynamical variables and p is a scalar parameter available for an external adjustment. We imagine that a scalar variable

$$y(t) = g(\boldsymbol{x}(t)), \tag{2.2}$$

which is a function of dynamic variables $\boldsymbol{x}(t)$, can be measured as the system output. Let us suppose that at $p = p_0 = 0$ the system has a UPO $\boldsymbol{x}_0(t)$ that satisfies $\dot{\boldsymbol{x}}_0 = \boldsymbol{f}(\boldsymbol{x}_0, 0, t)$ and $\boldsymbol{x}_0(t + T) = \boldsymbol{x}_0(t)$, where T is the period of the UPO. Here, the value

of the parameter p_0 is fixed to zero without loss of generality. To stabilize the UPO, we consider two continuous time feedback techniques, the PFC and the DFC, both introduced by Pyragas (1992).

The PFC uses the periodic reference signal

$$y_0(t) = g(\boldsymbol{x}_0(t)), \tag{2.3}$$

which corresponds to the system output if it would move along the target UPO. For chaotic systems, this periodic signal can be reconstructed from the chaotic output $y(t)$, using the standard methods for extracting UPOs from chaotic time-series data (Lathrop & Kostelich 1989; So *et al.* 1996). The control is achieved via adjusting the system parameter by a proportional feedback

$$p(t) = G[y_0(t) - y(t)], \tag{2.4}$$

where G is the control gain. If the stabilization is successful, the feedback perturbation $p(t)$ vanishes. The experimental implementation of this method is difficult since it is not simply to reconstruct the UPO from the experimental data.

A more convenient method for the experimental implementation is the DFC, which can be derived from the PFC by replacing the periodic reference signal $y_0(t)$ with the delayed output signal $y(t-T)$ (Pyragas 1992),

$$p(t) = K[y(t-T) - y(t)]. \tag{2.5}$$

Here, we exchanged the notation of the feedback gain with K to make it different from that of the proportional feedback. The delayed feedback perturbation in equation (2.5) also vanishes, provided the target UPO is stabilized. The DFC uses the delayed output $y(t-T)$ as the reference signal and the necessity of the UPO reconstruction is avoided. This feature determines the main advantage of the DFC over the PFC.

Hereafter, we shall consider a more general (extended) version of the DFC, the EDFC, in which a sum of states at integer multiples in the past is used (Socolar *et al.* 1994),

$$p(t) = K\left[(1-R)\sum_{n=1}^{\infty} R^{n-1} y(t-nT) - y(t)\right]. \tag{2.6}$$

The sum represents a geometric series with the parameter $|R|<1$ that determines the relative importance of past differences. For $R=0$, the EDFC transforms to the original DFC. The extended method is superior to the original in that it can stabilize UPOs of higher periods and with larger FEs. For experimental implementation, it is important that the infinite sum in equation (2.6) can be generated using only single time-delay element in the feedback loop.

The success of the above methods can be predicted by a linear stability analysis of the target orbit. For the PFC method, the small deviations from the UPO $\delta\boldsymbol{x}(t) = \boldsymbol{x}(t) - \boldsymbol{x}_0(t)$ are described by variational equation

$$\delta\dot{\boldsymbol{x}} = [\boldsymbol{A}(t) + G\boldsymbol{B}(t)]\delta\boldsymbol{x}, \tag{2.7}$$

where $\boldsymbol{A}(t)=\boldsymbol{A}(t+T)$ and $\boldsymbol{B}(t)=\boldsymbol{B}(t+T)$ are both T-periodic $m\times m$ matrices

$$\boldsymbol{A}(t) = D_1\boldsymbol{f}(\boldsymbol{x_0}(t),0,t), \tag{2.8a}$$

$$\boldsymbol{B}(t) = D_2\boldsymbol{f}(\boldsymbol{x}_0(t),0,t)\otimes Dg(\boldsymbol{x}_0(t)). \tag{2.8b}$$

Here, D_1 (D_2) denotes the vector (scalar) derivative with respect to the first (second) argument. The matrix $\boldsymbol{A}(t)$ defines the stability properties of the UPO of the free system and $\boldsymbol{B}(t)$ is the control matrix that contains all the details on the coupling of the control force.

Solutions of equation (2.7) can be decomposed into eigenfunctions according to the Floquet theory,

$$\delta\boldsymbol{x} = \exp(\Lambda t)\boldsymbol{u}(t), \quad \boldsymbol{u}(t) = \boldsymbol{u}(t+T), \tag{2.9}$$

where Λ is the FE. The spectrum of the FEs can be obtained with the help of the fundamental $m\times m$ matrix $\Phi(G,t)$ that is defined by equalities

$$\dot{\Phi}(G,t) = [A(t)+GB(t)]\Phi(G,t), \quad \Phi(G,0)=I. \tag{2.10}$$

For any initial condition $\boldsymbol{x}_{\mathrm{in}}$, the solution of equation (2.7) can be expressed with this matrix, $\boldsymbol{x}(t)=\Phi(G,t)\boldsymbol{x}_{\mathrm{in}}$. Combining this equality with equation (2.9), one obtains the system $[\Phi(G,T)-\exp(\Lambda T)I]\boldsymbol{x}_{\mathrm{in}}=0$ that yields the desired eigensolutions. The characteristic equation for the FEs reads

$$\det[\Phi(G,T)-\exp(\Lambda T)I]=0. \tag{2.11}$$

It defines m FEs Λ_j (or FMs $\mu_j=\exp(\Lambda_j T)$), $j=1,\ldots,m$, which are the functions of the control gain G,

$$\Lambda_j = F_j(G), \quad j=1,\ldots,m. \tag{2.12}$$

The values $F_j(0)$ are the FEs of the free system. By assumption, at least one FE of the free UPO has a positive real part. The PFC is successful if the real parts of all eigenvalues are negative, $\mathrm{Re}\,F_j(G)<0$, $j=1,\ldots,m$ in some interval of the parameter G.

Consider, next, the stability problem for the EDFC. The variational equation in this case reads

$$\delta\dot{\boldsymbol{x}} = \boldsymbol{A}(t)\delta\boldsymbol{x}(t) + K\boldsymbol{B}(t)\left[(1-R)\sum_{n=1}^{\infty}R^{n-1}\delta\boldsymbol{x}(t-nT)-\delta\boldsymbol{x}(t)\right]. \tag{2.13}$$

The delay terms can be eliminated owing to equation (2.9), $\delta\boldsymbol{x}(t-nT)=\exp(-n\Lambda T)\delta\boldsymbol{x}(t)$. As a result, the problem reduces to the system of ordinary differential equations, similar to equation (2.7),

$$\delta\dot{\boldsymbol{x}} = [\boldsymbol{A}(t)+KH(\Lambda)\boldsymbol{B}(t)]\delta\boldsymbol{x}, \tag{2.14}$$

where

$$H(\Lambda) = \frac{1-\exp(-\Lambda T)}{1-R\exp(-\Lambda T)}, \tag{2.15}$$

is the transfer function of the extended delayed feedback controller. Equations (2.7) and (2.14) have the same structure, defined by the matrices $\boldsymbol{A}(t)$ and $\boldsymbol{B}(t)$, and differ only by the value of the control gain. The equations become identical if we substitute $G = KH(\Lambda)$. The price one has to pay for the elimination of the delay terms is that the characteristic equation defining the FEs of the EDFC depends on the FEs itself,

$$\det[\Phi(KH(\Lambda), T) - \exp(\Lambda T) I] = 0. \tag{2.16}$$

Nevertheless, we can take advantage of the linear stability analysis for the PFC in order to predict the stability of the system controlled by time-delayed feedback. Suppose the functions $F_j(G)$ defining the FEs for the PFC are known, then the FEs of the UPO controlled by time-delayed feedback can be obtained through solution of the transcendental equation

$$\Lambda = F_j(KH(\Lambda)), \quad j = 1, \ldots, m. \tag{2.17}$$

Though a similar reduction of the EDFC variational equation has been considered by Bleich & Socolar (1996) and Just *et al.* (1997, 1999, 2000), here, we emphasize the physical meaning of the functions $F_j(G)$, namely, these functions describe the dependence of the FEs on the control gain in the case of the PFC.

In the general case, the analysis of the transcendental equation (2.17) is not a simple task owing to several reasons. First, the analytical expressions of the functions $F_j(G)$ are usually unknown and can be evaluated only numerically. Second, each FE of the free system $F_j(0)$ yields an infinite number of distinct FEs at $K \neq 0$; different eigenvalue branches that originate from different exponents of the free system may hibridizate or cross so that the branches originating from initially stable FEs may become dominant in some intervals of the parameter K (Just *et al.* 2000). Third, the functions F_j in the proportional feedback technique are defined for the real-valued argument G; however, we may need knowledge of these functions for the complex values of the argument $KH(\Lambda)$ when considering the solutions of equation (2.17).

In spite of the above difficulties that may emerge generally, there are many specific, practically important problems for which the most important information on the EDFC performance can be simply extracted from equations (2.15) and (2.17). Such problems cover low-dimensional systems whose UPOs arise from a period-doubling bifurcation.

In what follows, we concentrate on special types of free orbits, namely, those that flip their neighbourhood during one turn. More specifically, we consider UPOs whose leading FM is real and negative, so that the corresponding FE obeys $\mathrm{Im} F_1(0) = \pi/T$. It means that the FE is placed on the boundary of the 'Brillouin zone'. Such FEs are likely to remain on the boundary under various perturbations; hence, the condition $\mathrm{Im} F_1(G) = \pi/T$ holds in some finite interval of the control gain $G \in [G_{\min}, G_{\max}]$, $G_{\min} < 0$, $G_{\max} > 0$. Subsequently, we shall see that the main properties of the EDFC can be extracted from the function $\mathrm{Re}\, F_1(G)$, with the argument G varying in the above interval.

Let us introduce the dimensionless function

$$\phi(G) = F_1(G) T - i\pi, \tag{2.18}$$

which describes the dependence of the real part of the leading FE on the control gain G for the PFC and is denoted by

$$\lambda = \Lambda T - i\pi, \tag{2.19}$$

the dimensionless FE of the EDFC shifted by the amount π along the complex axes. Then, from equations (2.15) and (2.17), we derive

$$\lambda = \phi(G), \tag{2.20a}$$

$$K = G\frac{1 + R\exp(-\phi(G))}{1 + \exp(-\phi(G))}. \tag{2.20b}$$

These equations define the parametric dependence λ versus K for the EDFC. Here, G is treated as an independent real-valued parameter and we suppose that G varies in the interval $[G_{\min}, G_{\max}]$, so that the leading exponent $F_1(G)$ associated with the PFC remains on the boundary of the Brillouin zone; thus, the variables λ, K and the function ϕ are all real valued.

To demonstrate the benefit of equations (2.20*a*) and (2.20*b*), let us derive the stability threshold of the UPO controlled by the extended time-delayed feedback. The stability of the periodic orbit changes when λ reverses the sign. From equation (2.20*a*), it follows that the function $\phi(G)$ has to vanish for some value $G = G_1$, $\phi(G_1) = 0$. The value of the control gain G_1 is nothing but the stability threshold of the UPO controlled by the proportional feedback. Then, from equation (2.20*b*), one obtains the stability threshold

$$K_1 = G_1(1 + R)/2, \tag{2.21}$$

for the extended time-delayed feedback. In §2*c*, we shall demonstrate how to derive other properties of the EDFC using the specific examples of chaotic systems, but first we consider general features of the EDFC for a simple example in which a linear approximation of the function $\phi(G)$ is assumed.

(*b*) *Properties of the extended delayed feedback control: simple example*

To demonstrate the main properties of the EDFC, let us suppose that the function $\phi(G)$, defining the FE for the proportional feedback, depends linearly on the control gain G (cf. Just *et al.* 1997, 1999),

$$\phi(G) = \lambda_0(1 - G/G_1). \tag{2.22}$$

Here, λ_0 denotes the dimensionless FE of the free system and G_1 the stability threshold of the UPO controlled by proportional feedback. Substituting approximation (2.22) into equations (2.20*a*) and (2.20*b*), one derives the characteristic equation

$$k = (\lambda_0 - \lambda)\frac{1 + R\exp(-\lambda)}{1 + \exp(-\lambda)} \equiv \psi(\lambda), \tag{2.23}$$

defining the FEs for the EDFC. Here, $k = K\lambda_0/G_1$ is the renormalized control gain of the extended time-delayed feedback. The periodic orbit is stable if all the roots of equation (2.23) are in the left half-plane $\mathrm{Re}\,\lambda < 0$. The characteristic root-locus diagrams and the dependence $\mathrm{Re}\,\lambda$ versus k for two different values of the parameter R are shown in figure 2. The zeros and poles of the $\psi(\lambda)$ function

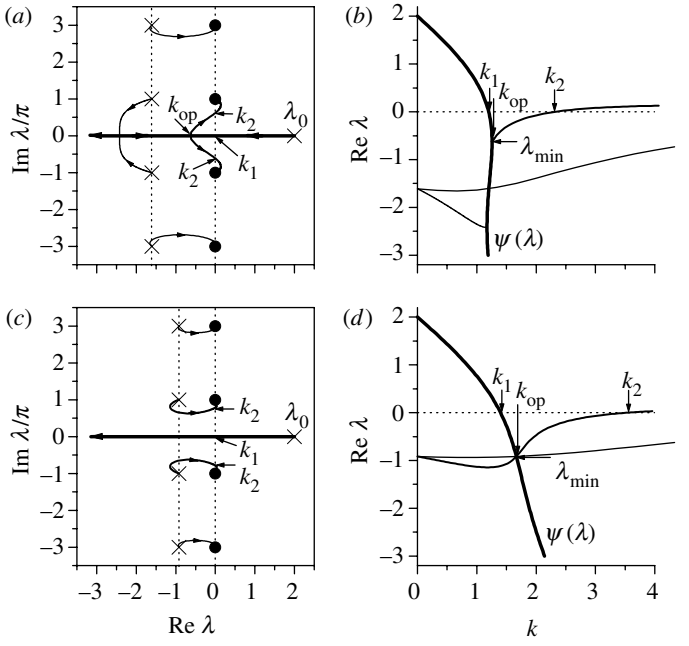

Figure 2. Root loci of equation (2.23) as k varies from 0 to ∞ and dependence Re λ versus k for $\lambda_0 = 2$ and two different values of the parameter R: (a) and (b) $R = 0.2 < R^\star$, (c) and (d) $R = 0.4 > R^\star$. The crosses and solid circles denote the location of roots at $k{=}0$ and $k \to \infty$, respectively. Thick solid lines in (b) and (c) symbolized by $\psi(\lambda)$ are the dependencies $k = \psi(\lambda)$ for real λ.

define the value of roots at $k{=}0$ and $k \to \infty$, respectively. For $k{=}0$ (an open-loop system), there is a real-valued root $\lambda = \lambda_0 > 0$ that corresponds to the FE of the free UPO and an infinite number of the complex roots $\lambda = \ln R + \mathrm{i}\pi n$, $n = \pm 1, \pm 3, \ldots$ in the left half-plane associated with the extended delayed feedback controller. For $k \to \infty$, the roots tend to the locations $\lambda = \mathrm{i}\pi n$, $n = \pm 1, \pm 3, \ldots$ determined by the poles of the $\psi(\lambda)$ function. For intermediate values of K, the roots can evolve by two different scenarios depending on the value of the parameter R.

If R is small enough ($R < R^\star$), the conjugate pair of the controller's roots $\lambda = \ln R \pm \mathrm{i}\pi$ collides on the real axes (figure 2a). After collision, one of these roots moves along the real axes toward $-\infty$, and another approaches the FE of the UPO, then collides with this FE at $k = k_{\mathrm{op}}$ and passes to the complex plane. Afterwards, this pair of complex conjugate roots move toward the points $\pm\mathrm{i}\pi$. At $k = k_2$, they cross into the right half-plane. In the interval $k_1 < k < k_2$, all roots of equation (2.23) are in the left half-plane and the UPO controlled by the extended time-delayed feedback is stable. The left boundary of the stability domain satisfies equation (2.21). For the renormalized value of the control gain, it reads

$$k_1 = \lambda_0(1 + R)/2. \tag{2.24}$$

An explicit analytical expression for the right boundary k_2 is unavailable. Inside the stability domain, there is an optimal value of the control gain $k = k_{\mathrm{op}}$, which for the fixed R provides the minimal value $\lambda_{\min}$ for the real part of the leading FE (figure 2b). To obtain the values k_{op} and $\lambda_{\min}$, it suffices to examine the properties of the function $\psi(\lambda)$ for the real values of the argument λ. The values k_{op} and $\lambda_{\min}$ are

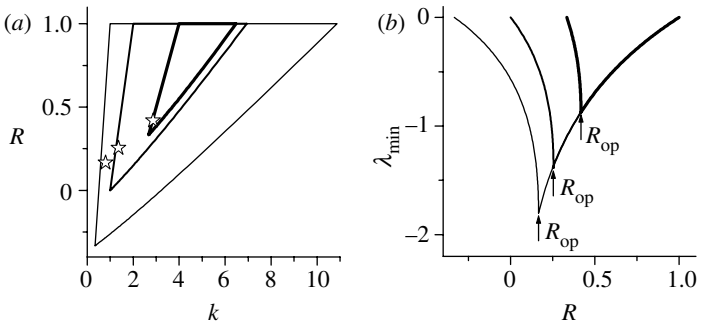

Figure 3. (*a*) Stability domains of equation (2.23) in the (k, R) plane and (*b*) dependence $\lambda_{\min}$ versus R for different values of $\lambda_0 = 1$, 2 and 4 (increasing line thickness corresponds to increasing values of λ_0). The stars inside the stability domains denote the optimal values $(k_{\rm op}, R_{\rm op})$.

conditioned by the maximum of this function and satisfy the equalities

$$\psi'(\lambda_{\min}) = 0, \quad k_{\rm op} = \psi(\lambda_{\min}). \tag{2.25}$$

The above scenario is valid when the function $\psi(\lambda)$ is at the maximum. The maximum disappears at $R = R^\star$ when it collides with the minimum of this function so that the conditions $\psi'(\lambda) = 0$ and $\psi''(\lambda) = 0$ are fulfilled. For $\lambda_0 = 2$, these conditions yield $R^\star \approx 0.255$.

Now, we consider an evolution of roots for $R > R^\star$ (figure 2*c*,*d*). In this case, the modes related to the controller and the UPO evolve independently from each other. The FE of the UPO moves along the real axes towards $-\infty$ without hibridizing with the modes of the controller. As previously, the left boundary k_1 of the stability domain is determined by equation (2.24). The right boundary k_2 is conditioned by the controller mode associated with the roots $\lambda = \ln R \pm i\pi$ at $k = 0$ that move towards $\lambda = \pm i\pi$ for $k \to \infty$. The optimal value $k_{\rm op}$ is defined by a simple intersection of the real part of this mode with the mode related to the UPO.

Stability domains of the periodic orbit in the plane of parameters (k, R) are shown in figure 3*a*. The left boundary of this domain is the straight line defined by equation (2.24). The right boundary is determined by parametric equations

$$k_2 = \frac{\lambda_0^2 + s^2}{\lambda_0 + s\cot(s/2)}, \quad R = \frac{\lambda_0 - s\cot(s/2)}{\lambda_0 + s\cot(s/2)}, \tag{2.26}$$

with the parameter s varying in the interval $[0, \pi]$. As is seen from the figure, the stability domain is smaller for the UPOs with a larger FE λ_0. Figure 3*b* shows the optimal properties of the EDFC, namely, the dependence $\lambda_{\min}$ versus R, where $\lambda_{\min}$ is the value of the leading Floquet mode evaluated at $k = k_{\rm op}$. This dependence possesses a minimum at $R = R_{\rm op} = R^\star$. Thus, for any given λ_0, there exists an optimal value of the parameter $R = R_{\rm op}$, which at $k = k_{\rm op}$ provides the fastest convergence of nearby trajectories to the target periodic orbit. For $R > R_{\rm op}$, the performance of the EDFC is adversely affected with the increase in R, since for R close to 1, the modes of the controller are damped out very slowly, $\mathrm{Re}\,\lambda = \ln R$.

In this section, we used an explicit analytical expression for the function $\phi(G)$ when analysing the stability properties of the UPO controlled by the extended time-delayed feedback. In the following sections, we consider a situation when

the function $\phi(G)$ is available only numerically and only for real values of the parameter G. We show that, in this case, the main stability characteristics of the system controlled by time-delayed feedback can be derived as well.

(c) *Demonstration for the Rössler system*

Let us consider the problem of stabilizing the period-one UPO of the Rössler (1976) system,

$$\begin{pmatrix} \dot{x}_1 \\ \dot{x}_2 \\ \dot{x}_3 \end{pmatrix} = \begin{pmatrix} -x_2 - x_3 \\ x_1 + a x_2 \\ b + (x_1 - c) x_3 \end{pmatrix} + p(t) \begin{pmatrix} 0 \\ 1 \\ 0 \end{pmatrix}. \tag{2.27}$$

Here, we suppose that the feedback perturbation $p(t)$ is applied only to the second equation of the Rössler system and the dynamic variable x_2 is an observable available at the system output, i.e. $y(t) = g(\boldsymbol{x}(t)) = x_2(t)$.

For parameter values, $a = 0.2$, $b = 0.2$ and $c = 5.7$, the free ($p(t) \equiv 0$) Rössler system exhibits chaotic behaviour. An approximate period of the period-one UPO $\boldsymbol{x}_0(t) = \boldsymbol{x}_0(t + T)$ embedded in a chaotic attractor is $T \approx 5.88$. Linearizing equation (2.27) around the UPO, one obtains explicit expressions for the matrices $\boldsymbol{A}(t)$ and $\boldsymbol{B}(t)$ defined in equation (2.8*a*) and (2.8*b*),

$$\boldsymbol{A}(t) = \begin{pmatrix} 0 & -1 & -1 \\ 1 & a & 0 \\ x_3^0(t) & 0 & x_1^0(t) - c \end{pmatrix}, \tag{2.28}$$

and $\boldsymbol{B} = \mathrm{diag}(0, -1, 0)$. Here, $x_j^0(t)$ denotes the jth component of the UPO.

First, we consider the system in equation (2.27) controlled by proportional feedback, when the perturbation $p(t)$ is defined by equation (2.4). By solving equations (2.10) and (2.11), we obtain three FEs, Λ_1, Λ_2 and Λ_3, as functions of the control gain G. The real parts of these functions are presented in figure 4*a*. The values of the FEs of the free ($G = 0$) UPO are $\Lambda_1 T = 0.876 + i\pi$, $\Lambda_2 T = 0$ and $\Lambda_3 T = -31.974 + i\pi$. Thus, the first and third FEs are located on the boundary of the Brillouin zone. The second, zero FE, is related to the translational symmetry that is general for any autonomous system. The dependence of the FEs on the control gain G is rather complex if it would be considered in a large interval of the parameter G. In figure 4*a*, we restricted ourselves with a small interval of the parameter $G \in [0, 0.67]$ in which all FEs do not change their imaginary parts, i.e. the FEs Λ_1 and Λ_3 remain on the boundary of the Brillouin zone, $\mathrm{Im}\,\Lambda_1 T = i\pi$, $\mathrm{Im}\,\Lambda_3 T = i\pi$ and Λ_2 remain real valued, and $\mathrm{Im}\,\Lambda_2 = 0$ for any G in the above interval. Any information on the behaviour of the leading FE Λ_1 or, more precisely, of the real-valued function $\phi(G) = \Lambda_1 T - i\pi$ in this interval will suffice to derive the main stability properties of the system controlled by time-delayed feedback.

The main information on the EDFC performance can be gained from parametric equations (2.20*a*) and (2.20*b*). They make possible a simple reconstruction of the relevant Floquet branch in the (K, λ) plane. This Floquet branch is shown in figure 4*b* for different values of the parameter R. Let us denote

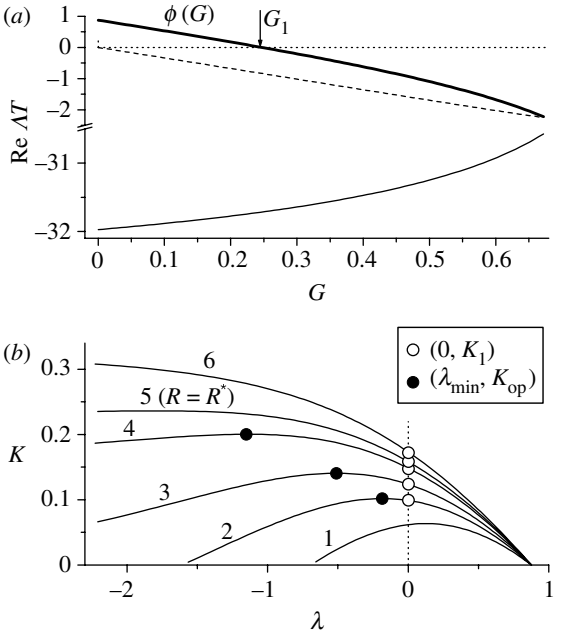

Figure 4. (*a*) FEs of the Rössler system under PFC as functions of the control gain G. Thick solid, thin broken and thin solid lines represent the functions $\Lambda_1 T - \mathrm{i}\pi$, $\Lambda_2 T$ (zero exponent) and $\Lambda_3 T - i\pi$, respectively. (*b*) Parametric dependence K versus λ defined by equations (2.20*a*) and (2.20*b*) for the EDFC. The numbers mark the curves with different values of the parameter R: (1) -0.5, (2) -0.2, (3) 0, (4) 0.2, (5) 0.28 and (6) 0.4. Solid circles show the maxima of the curves and open circles indicate their intersections with the line $\lambda = 0$.

the dependence K versus λ corresponding to this branch by a function ψ, $K = \psi(\lambda)$. Formally, an explicit expression for this function can be written in the form

$$\psi(\lambda) = \phi^{-1}(\lambda)\frac{1 + R\exp(-\lambda)}{1 + \exp(-\lambda)}, \tag{2.29}$$

where ϕ^{-1} denotes the inverse function of $\phi(G)$. More convenient for graphical representation of this dependence is, of course, the parametric form (2.20*a*) and (2.20*b*). The EDFC will be successful if the maximum of this function is located in the region $\lambda < 0$. Then the maximum defines the minimal value of the leading FE $\lambda_{\min}$ for the EDFC, and $K_{\mathrm{op}} = \psi(\lambda_{\min})$ is the optimal value of the control gain at which the fastest convergence of the nearby trajectories to the target orbit is attained. From figure 4*b*, it is evident that the delayed feedback controller should gain in performance through an increase in the parameter R, since the maximum of the $\psi(\lambda)$ function moves to the left. At $R = R^{\star} \approx 0.28$, the maximum disappears. For $R > R^{\star}$, it is difficult to predict the optimal characteristics of the EDFC. In §2*b*, we have established that, in this case, the value $\lambda_{\min}$ is determined by the intersection of different Floquet branches.

The left boundary of the stability domain is defined by the equality $K_1 = \psi(0)$ (figure 4*b*) or alternatively by equation (2.21), $K_1 = G_1(1 + R)/2$. This relationship between the stability thresholds of the periodic orbit controlled by the PFC and the EDFC is rather universal and is valid for systems whose leading

FE of the UPO is placed on the boundary of the Brillouin zone. It is interesting to note that the stability threshold for the original DFC ($R=0$) is equal to one half of the threshold in the case of the PFC, $K_1 = G_1/2$.

An evaluation of the right boundary K_2 of the stability domain is a more intricate problem. Nevertheless, for the parameter $R < R^\star$, it can be successfully solved by means of an analytical continuation of the function $\psi(\lambda)$ on the complex region. For this purpose, we expend the function $\psi(\lambda)$, at the point $\lambda = \lambda_{\min}$, into power series

$$\psi(\lambda) = K_{\rm op} + \sum_{n=2}^{N+1} \alpha_n (\lambda - \lambda_{\min})^n. \tag{2.30}$$

We evaluate the coefficients α_n, numerically, by the least-squares fitting. In this procedure, we use the knowledge of numerical values of the function $\psi(\lambda_m)$, $m = 1, \ldots, M$ in $M > N$ points placed on the real axes and solve a corresponding system of N linear equations. To extend the Floquet branch to the region $K > K_{\rm op}$, we have to solve the equation $K = \psi(\lambda)$ for the complex argument λ. Substituting $\lambda - \lambda_{\min} = r \exp(i\varphi)$ into equation (2.30), we obtain

$$\sum_{n=2}^{N+1} \alpha_n r^n \sin n\varphi = 0, \tag{2.31a}$$

$$K = K_{\rm op} + \sum_{n=2}^{N+1} \alpha_n r^n \cos n\varphi, \tag{2.31b}$$

$$\mathrm{Re}\ \lambda = \lambda_{\min} + r \cos\varphi, \tag{2.31c}$$

$$\mathrm{Im}\lambda = r \sin\varphi. \tag{2.31d}$$

Let us suppose that r is an independent parameter. By solving equation (2.31*a*), we can determine φ as a function of r, $\varphi = \varphi(r)$. Then, equations (2.31*b*), (2.31*c*) and (2.31*d*) define the parametric dependencies, $\mathrm{Re}\,\lambda$ versus K and $\mathrm{Im}\lambda$ versus K, respectively.

Figure 5 shows the dependence of the leading FEs on the control gain K for the EDFC. The thick solid line represents the most important Floquet branch that conditions the main stability properties of the system. It is described by the function $K = \psi(\lambda)$ with the real argument λ. It should be noted that the same function has been depicted in figure 4*b* for inverted axes. For $R < R^\star$, this branch originates an additional sub-branch, which starts at the point $(K_{\rm op}, \lambda_{\min})$ and spreads to the region $K > K_{\rm op}$. The sub-branch is described by equations (2.31*a*)–(2.31*d*), which results from an analytical continuation of the function $\psi(\lambda)$ on the complex plane. This sub-branch is leading in the $K > K_{\rm op}$ region and its intersections with the line $\lambda = 0$ defines the right boundary K_2 of the stability domain. In figure 5*a*,*b*, the sub-branches are shown by solid lines. As seen from the figures, the Floquet sub-branches obtained by means of an analytical continuation are in good agreement with the 'exact' solutions evaluated from the complete system of equations (2.10), (2.15) and (2.16).

For $R > R^\star$, the maximum in the function $\psi(\lambda)$ disappears and the Floquet branch that originated from the eigenvalues $\lambda = \ln R \pm i\pi$ of the controller (see §2*b*), becomes dominant in the $K > K_{\rm op}$ region. This Floquet branch as well

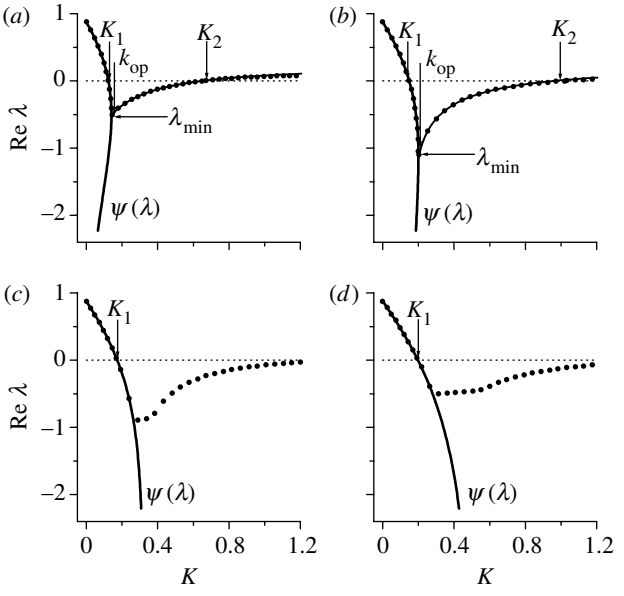

Figure 5. Leading FEs of the Rössler system under EDFC as functions of the control gain K for different values of the parameter R. (a) $R=0.1$, (b) $R=0.2$, (c) $R=0.4$ and (d) $R=0.6$. Thick solid lines symbolized by $\psi(\lambda)$ show the dependence $K=\psi(\lambda)$ for real λ. Solid lines in the region $K>K_{\mathrm{op}}$ are defined from equations (2.31a)–(2.31d). The number of terms in series (2.30) is $N=15$. Solid circles denote the 'exact' solutions obtained from complete system of equations (2.10), (2.15) and (2.16).

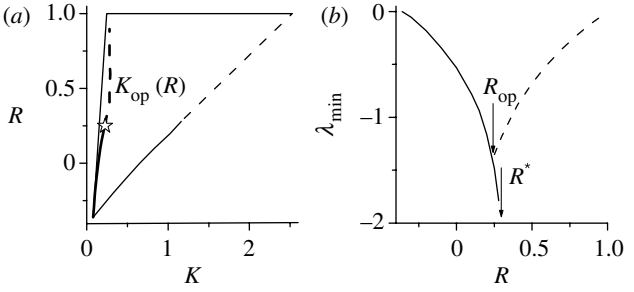

Figure 6. (a) Stability domain of the period-one UPO of the Rössler system under EDFC. The thick curve inside the domain shows the dependence K_{op} versus R. The star marks the optimal point $(K_{\mathrm{op}}, R_{\mathrm{op}})$. ($b$) Minimal value λ_{min} of the leading FE as a function of the parameter R. In both figures, solid and broken lines denote the solutions obtained from equations (2.20a), (2.20b), (2.10), (2.15) and (2.16), respectively.

as the intersection point $(K_{\mathrm{op}}, \lambda_{\mathrm{min}})$ are unpredictable via a simple analysis. It can be determined by solving the complete system of equations (2.10), (2.15) and (2.16). In figure 5c,d, these solutions are shown by dots.

Figure 6 demonstrates the amount of information one can gain via a simple analysis of parametric equations (2.20a) and (2.20b). These equations allow us to construct the stability domain in the (K, R) plane almost completely. The most important information on optimal properties of the EDFC can be obtained from these equations as well. The thick curve in the stability domain shows the dependence of the optimal value of the control gain K_{op} on the parameter R.

The star marks an optimal choice of both parameters $(K_{\rm op}, R_{\rm op})$, which provide the fastest decay of perturbations. Figure 6*b* shows how the decay rate $\lambda_{\min}$ attained at the optimal value of the control gain $K_{\rm op}$ depends on the parameter R. The left part of this dependence is simply defined by the maximum of the function $\psi(\lambda)$, while the right part is determined by intersection of different Floquet branches and can be evaluated only with the complete system of equations (2.10), (2.15) and (2.16). Unlike the simple model considered in §2*b*, here, the intersection occurs before the maximum in the function $\psi(\lambda)$ disappears, i.e. at $R = R_{\rm op} < R^{\star}$. Nevertheless, the value $R^{\star}$ gives a good estimate for the optimal value of the parameter R, since $R^{\star}$ is close to $R_{\rm op}$.

3. Stabilization of torsion-free periodic orbits

Most investigations on the DFC method are restricted to the consideration of UPOs arising from a flip bifurcation. The leading FM of such orbits is real and negative (or the corresponding FE lies on the boundary of the Brillouin zone, $\mathrm{Im}\Lambda = \pi/T$). Such a consideration is motivated by the fact that the usual DFC and EDFC methods work only for the orbits with a finite torsion, when the leading FE obeys $\mathrm{Im}\Lambda \neq 0$. Unsuitability of the DFC technique to stabilize torsion-free orbits ($\mathrm{Im}\Lambda = 0$) has been considered, over several years, as a main limitation of the method (Ushio 1996; Just *et al.* 1997; Nakajima 1997*b*; Nakajima & Ueda 1998*a*). More precisely, the limitation is that any UPOs with an odd number of real FMs greater than unity can never be stabilized by the DFC. This limitation can be explained by the bifurcation theory as follows. When a UPO with an odd number of real FMs greater than unity is stabilized, one of such multipliers must cross the unit circle on the real axes in the complex plane. Such a situation corresponds to a tangent bifurcation, which is accompanied with a coalescence of T-periodic orbits. However, this contradicts the fact that DFC perturbation does not change the location of T-periodic orbits when the feedback gain varies, because the feedback term vanishes for T-periodic orbits.

Here, we describe an unstable delayed feedback controller that can overcome the limitation (Pyragas 2001). The idea is to artificially enlarge a set of real multipliers greater than unity to an even number, by introducing an unstable degree of freedom into a feedback loop.

(*a*) *Simple example: extended delayed feedback control for* $R>1$

First, we illustrate the idea for a simple unstable discrete-time system $y_{n+1} = \mu_s y_n$, $\mu_s > 1$, controlled by the EDFC

$$y_{n+1} = \mu_s y_n - K F_n, \tag{3.1}$$

$$F_n = y_n - y_{n-1} + R F_{n-1}. \tag{3.2}$$

The free system $y_{n+1} = \mu_s y_n$ has an unstable fixed point $y^{\star} = 0$ with the only real eigenvalue $\mu_s > 1$ and, in accordance with the above limitation, cannot be stabilized by the EDFC for any values of the feedback gain K. This is so, if the EDFC is stable, i.e. if the parameter R in equation (3.2) satisfies the inequality

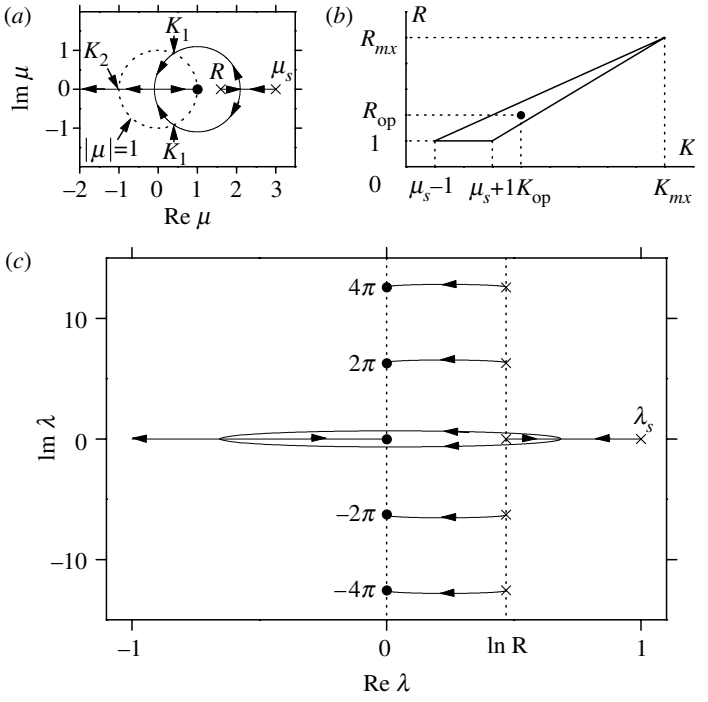

Figure 7. Performance of (*a* and *b*) discrete and (*c*) continuous EDFC for $R>1$. (*a*) Root loci of equation (3.3) at $\mu_s=3$, $R=1.6$ as K varies from 0 to ∞. (*b*) Stability domain of equations (3.1) and (3.2) in the (K, R) plane; $K_{mx}=(\mu_s+1)^2/(\mu_s-1)$, $R_{mx}=(\mu_s+3)/(\mu_s-1)$. (*c*) Root loci of equation (3.6) at $\lambda_s=1$, $R=1.6$. The crosses and solid circles denote the location of roots at $K=0$ and $K\to\infty$, respectively.

$|R|<1$. Only this case has been considered in the literature. However, it is easy to show that the unstable controller with the parameter $R>1$ can stabilize this system. Using the ansatz y_n, $F_n\propto\mu^n$, one obtains the characteristic equation

$$(\mu-\mu_s)(\mu-R)+K(\mu-1)=0, \tag{3.3}$$

defining the eigenvalues μ of the closed-loop system in equations (3.1) and (3.2). The system is stable if both roots $\mu=\mu_{1,2}$ of equation (3.3) are inside the unit circle of the μ complex plain, $|\mu_{1,2}|<1$. Figure 7*a* shows the characteristic root-locus diagram for $R>1$, as the parameter K varies from 0 to ∞. For $K=0$, there are two real eigenvalues greater than unity, $\mu_1=\mu_s$ and $\mu_2=R$, which correspond to two independent subsystems of equation (3.1) and (3.2), respectively; this means that both the controlled system and the controller are unstable. With the increase in K, the eigenvalues approach each other on the real axes, collide and pass to the complex plane. At $K=K_1\equiv\mu_sR-1$, they cross the unit circle $|\mu|=1$ symmetrically. Then, both eigenvalues move inside this circle, collide again on the real axes and one of them leaves the circle at $K=K_2\equiv(\mu_s+1)(R+1)/2$. In the interval $K_1<K<K_2$, the closed-loop system in equations (3.1) and (3.2) is stable. By a proper choice of the parameters R and K, one can stabilize the fixed point with an arbitrarily large eigenvalue μ_s. The corresponding stability domain is shown in figure 7*b*. For a given value μ_s, there

is an optimal choice of the parameters $R=R_{\rm op}\equiv\mu_s/(\mu_s-1)$ and $K=K_{\rm op}\equiv\mu_s R_{\rm op}$, leading to zero eigenvalues, $\mu_1=\mu_2=0$, such that the system approaches the fixed point in finite time.

It seems attractive to apply the EDFC with the parameter $R>1$ for continuous-time systems. Unfortunately, this idea fails. As an illustration, let us consider a continuous time version of equations (3.1) and (3.2),

$$\dot{y}(t) = \lambda_s y(t) - KF(t), \tag{3.4}$$

$$F(t) = y(t) - y(t-\tau) + RF(t-\tau), \tag{3.5}$$

where $\lambda_s>0$ is the characteristic exponent of the free system $\dot{y}=\lambda_s y$ and τ is the delay time. By a suitable rescaling, one can eliminate one of the parameters in equations (3.4) and (3.5). Thus, without a loss of generality, we can take $\tau=1$. Equations (3.4) and (3.5) can be solved by the Laplace transform or simply by the substitution $y(t)$, $F(t)\propto \mathrm{e}^{\lambda t}$ that yields the characteristic equation

$$1 + K\frac{1-\exp(-\lambda)}{1-R\exp(-\lambda)}\,\frac{1}{\lambda-\lambda_s} = 0. \tag{3.6}$$

In terms of the control theory, equation (3.6) defines the poles of the closed-loop transfer function. The first and the second fractions in equation (3.6) correspond to the EDFC and plant transfer functions, respectively. The closed-loop system in equation (3.4) and (3.5) is stable if all the roots of equation (3.6) are in the left half-plane, Re $\lambda<0$. The characteristic root-locus diagram for $R>1$ is shown in figure 7*c*. When K varies from 0 to ∞, the EDFC roots move in the right half-plane from locations $\lambda=\ln R+2\pi i n$ to $\lambda=2\pi i n$, for $n=\pm1,\pm2\ldots$. Thus, the continuous time EDFC with the parameter $R>1$ has an infinite number of unstable degrees of freedom and many of them remain unstable in the closed-loop system for any K.

(*b*) *Usual extended delayed feedback control supplemented by an unstable degree of freedom*

Hereafter, we shall use the usual EDFC at $0\leq R<1$; however, we introduce an additional unstable degree of freedom into a feedback loop. More specifically, for a dynamical system $\dot{\boldsymbol{x}}=\boldsymbol{f}(\boldsymbol{x},p)$ with a measurable scalar variable $y(t)=g(\boldsymbol{x}(t))$ and a UPO of period τ at $p=p_0=0$, we propose to adjust an available system parameter p by a feedback signal $p(t)=KF_u(t)$ of the following form:

$$F_u(t) = F(t) + w(t), \tag{3.7}$$

$$\dot{w}(t) = \lambda_c^0 w(t) + (\lambda_c^0-\lambda_c^\infty)F(t), \tag{3.8}$$

$$F(t) = y(t) - (1-R)\sum_{k=1}^{\infty} R^{k-1} y(t-k\tau), \tag{3.9}$$

where $F(t)$ is the usual EDFC described by equation (3.5) or equivalently by equation (3.9). Equation (3.8) defines an additional unstable degree of freedom with parameters $\lambda_c^0>0$ and $\lambda_c^\infty<0$. We emphasize that, whenever the

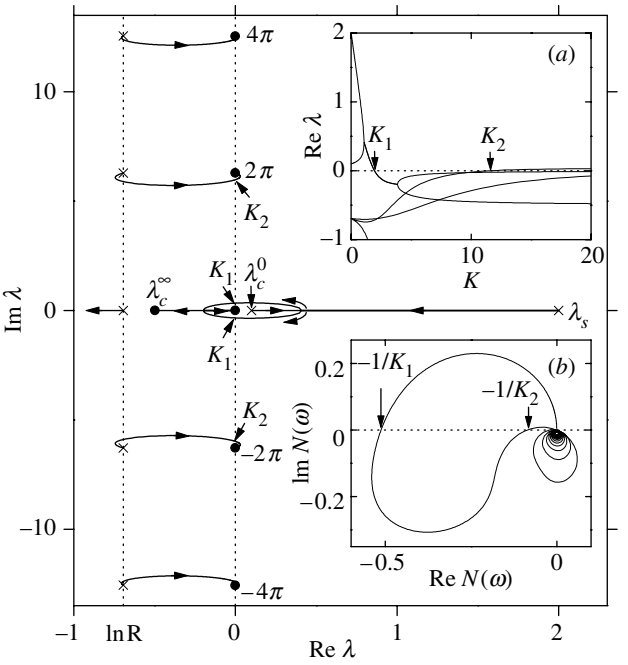

Figure 8. Root loci of equation (3.11) at $\lambda_s = 2$, $\lambda_c^0 = 0.1$, $\lambda_c^\infty = -0.5$, $R = 0.5$. The insets (*a*) and (*b*) show $\mathrm{Re}\,\lambda$ versus K and the Nyquist plot, respectively. The boundaries of the stability domain are $K_1 \approx 1.95$ and $K_2 \approx 11.6$.

stabilization is successful, the variables $F(t)$ and $w(t)$ vanish, and hence the feedback force $F_u(t)$ vanishes. We refer to the feedback laws (3.7)–(3.9) as unstable extended delayed feedback controls (UEDFCs).

To get an insight into how the UEDFC works, let us again consider the problem of stabilizing the fixed point

$$\dot{y} = \lambda_s y - KF_u(t), \tag{3.10}$$

where $F_u(t)$ is defined by equations (3.7)–(3.9) and $\lambda_s > 0$. Here, as well as in a previous example, we can take $\tau = 1$ without a loss of generality. Now, the characteristic equation reads

$$1 + KQ(\lambda) = 0, \tag{3.11}$$

$$Q(\lambda) \equiv \frac{\lambda - \lambda_c^\infty}{\lambda - \lambda_c^0} \frac{1 - \exp(-\lambda)}{1 - R\exp(-\lambda)} \frac{1}{\lambda - \lambda_s}. \tag{3.12}$$

The first fraction in equation (3.12) corresponds to the transfer function of an additional unstable degree of freedom. Root loci of equation (3.11) are shown in figure 8. The poles and zeros of the Q-function define the value of roots at $K = 0$ and $K \to \infty$, respectively. Now at $K = 0$, the EDFC roots $\lambda = \ln R + 2\pi i n$, $n = 0, \pm 1, \ldots$, are in the left half-plane. The only root λ_c^0 associated with an additional unstable degree of freedom is in the right half-plane. Root λ_c^0 and the root λ_s of the fixed point, collide on the real axes, pass to the complex plane and cross into the left half-plane at $K = K_1$. For $K_1 < K < K_2$, all roots of equation (3.11) satisfy the inequality $\mathrm{Re}\,\lambda < 0$, and the closed-loop system (3.7)–(3.10) is

stable. The stability is destroyed at $K=K_2$ when the EDFC roots $\lambda=\ln R\pm 2\pi i$ in the second Brillouin zone cross into Re $\lambda>0$. The dependence of the five largest Re λ on K is shown in the inset (a) of figure 8. The inset (b) shows the Nyquist plot, i.e. a parametric plot Re $N(\omega)$ versus Im$N(\omega)$ for $\omega\in[0,\infty]$, where $N(\omega)\equiv Q(i\omega)$. The Nyquist plot provides the simplest way of determining the stability domain, it crosses the real axes at Re $N=-1/K_1$ and $-1/K_2$.

As a more involved example, let us consider the Lorenz (1963) system under the UEDFC,

$$\begin{pmatrix}\dot{x}\\ \dot{y}\\ \dot{z}\end{pmatrix}=\begin{pmatrix}-\sigma x+\sigma y\\ rx-y-xz\\ xy-bz\end{pmatrix}-KF_u(t)\begin{pmatrix}0\\ 1\\ 0\end{pmatrix}. \tag{3.13}$$

We assume that the output variable is y and the feedback force $F_u(t)$ (equations (3.7)–(3.9)) perturbs only the second equation of the Lorenz system. The variables of the Lorenz system are denoted by $\boldsymbol{\rho}=(x,y,z)$ and those extended with the controller variable w by $\boldsymbol{\xi}=(\boldsymbol{\rho},w)^{\mathrm{T}}$. For the parameters $\sigma=10$, $r=28$ and $b=8/3$, the free ($K=0$) Lorenz system has a period-one UPO, $\boldsymbol{\rho}_0(t)\equiv(x_0,y_0,z_0)=\boldsymbol{\rho}_0(t+\tau)$, with the period $\tau\approx 1.5586$ and all real FMs, $\mu_1\approx 4.714$, $\mu_2=1$ and $\mu_3\approx 1.19\times 10^{-10}$. This orbit cannot be stabilized by usual DFC or EDFC, since only one FM is greater than unity. The ability of the UEDFC to stabilize this orbit can be verified by a linear analysis of equations (3.13) and (3.7)–(3.9). Small deviations $\delta\boldsymbol{\xi}=\boldsymbol{\xi}-\boldsymbol{\xi}_0$ from the periodic solution $\boldsymbol{\xi}_0(t)\equiv(\boldsymbol{\rho}_0,0)^{\mathrm{T}}=\boldsymbol{\xi}_0(t+\tau)$ may be decomposed into eigenfunctions according to the Floquet theory, $\delta\boldsymbol{\xi}=\mathrm{e}^{\lambda t}\boldsymbol{u}$, $\boldsymbol{u}(t)=\boldsymbol{u}(t+\tau)$, where λ is the FE. The Floquet decomposition yields linear periodically time-dependent equations $\delta\dot{\boldsymbol{\xi}}=A\delta\boldsymbol{\xi}$ with the boundary condition $\delta\boldsymbol{\xi}(\tau)=\mathrm{e}^{\lambda\tau}\delta\boldsymbol{\xi}(0)$, where

$$\boldsymbol{A}=\begin{pmatrix}-\sigma & \sigma & 0 & 0\\ r-z_0(t) & -(1+KH) & -x_0(t) & -K\\ y_0(t) & x_0(t) & -b & 0\\ 0 & (\lambda_c^0-\lambda_c^\infty)H & 0 & \lambda_c^0\end{pmatrix}. \tag{3.14}$$

Owing to equality $\delta y(t-k\tau)=\mathrm{e}^{-k\lambda\tau}\delta y(t)$, the delay terms in equation (3.9) are eliminated, and the equation is transformed to $\delta F(t)=H\delta y(t)$, where

$$H=H(\lambda)=(1-\exp(-\lambda\tau))/(1-R\exp(-\lambda\tau)), \tag{3.15}$$

is the transfer function of the EDFC. The price for this simplification is that the Jacobian $\boldsymbol{A}$, defining the exponents λ, depends on λ itself. The eigenvalue problem may be solved with a fundamental matrix $\boldsymbol{\Phi}_t$ that satisfies

$$\dot{\boldsymbol{\Phi}}_t=\boldsymbol{A}\boldsymbol{\Phi}_t,\quad \boldsymbol{\Phi}_0=I. \tag{3.16}$$

The eigenvalues of $\boldsymbol{\Phi}_\tau$ define the desired exponents,

$$\det[\boldsymbol{\Phi}_\tau(H)-\mathrm{e}^{\lambda\tau}I]=0. \tag{3.17}$$

We emphasize the dependence of $\boldsymbol{\Phi}_\tau$ on H conditioned by the dependence of $\boldsymbol{A}$ on H. Thus, by solving equations (3.15)–(3.17), one can define the FEs λ (or multipliers $\mu=\mathrm{e}^{\lambda\tau}$) of the Lorenz system under the UEDFC. Figure 9a shows the dependence of the six largest Re λ on K. There is an interval $K_1<K<K_2$, where

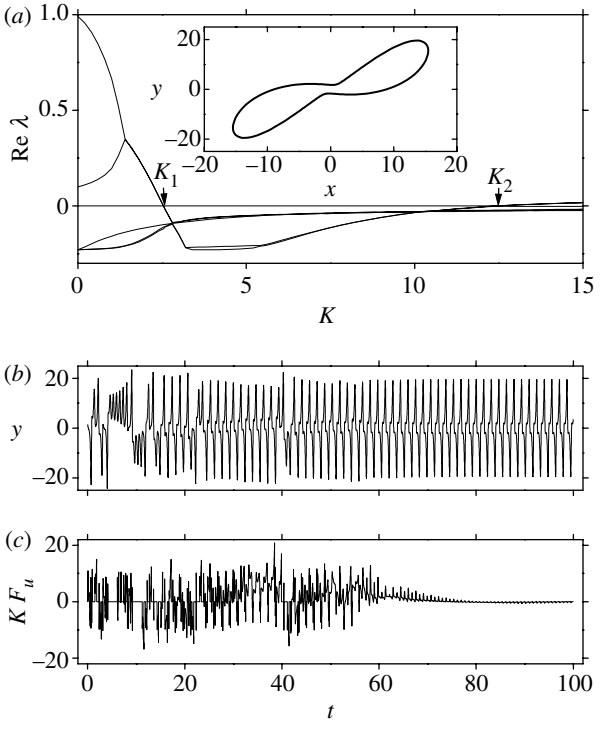

Figure 9. Stabilization of a UPO of the Lorenz system. (*a*) Six largest Re λ versus K. The boundaries of the stability domain are $K_1 \approx 2.54$ and $K_2 \approx 12.3$. The inset shows the (x, y) projection of the UPO. Parts (*b*) and (*c*) show the dynamics of $y(t)$ and $F_u(t)$ obtained from equations (3.13) and (3.7)–(3.9). The parameters are: $\lambda_c^0 = 0.1$, $\lambda_c^\infty = -2$, $R = 0.7$, $K = 3.5$, $\varepsilon = 3$ and $\lambda_r = 10$.

the real parts of all exponents are negative. Basically, figure 9*a* shows the results similar to those presented in figure 8*a*. The unstable exponent λ_1 of a UPO and the unstable eigenvalue λ_c^0 of the controller collide on the real axes and pass into the complex plane providing a UPO with a finite torsion. Then, this pair of complex conjugate exponents crosses into domain Re $\lambda < 0$, just as it does in the simple model of equation (3.10).

Direct integration of the nonlinear equations (3.13) and (3.7)–(3.9) confirms the results of linear analysis. Figure 9*b*,*c* shows a successful stabilization of the target UPO with an asymptotically vanishing perturbation. In this analysis, we used a restricted perturbation similar to that in the previous paper (Pyragas 1992). For $|F(t)| < \varepsilon$, the control force $F_u(t)$ is calculated from equations (3.7)–(3.9); however, for $|F(t)| > \varepsilon$, the control is switched off, $F_u(t) = 0$, and the unstable variable w is dropped off by replacing equation (3.8) with the relaxation equation $\dot{w} = -\lambda_r w$, $\lambda_r > 0$.

4. Conclusions

The aim of this paper was to review experimental implementations, applications for theoretical models and modifications of the time-delayed feedback control method and to present some recent theoretical ideas in this field.

In §2, we have demonstrated how to use the relationship between the Floquet spectra of the system controlled by proportional and time-delayed feedback in order to obtain the main stability properties of the system, controlled by time-delayed feedback. Our consideration has been restricted to low-dimensional systems, whose UPOs originated from a period-doubling bifurcation. These orbits flip their neighbourhood during one turn, so that the leading FE is placed on the boundary of the Brillouin zone. Knowing the dependence of this exponent on the control gain for the PFC, one can simply construct the relevant Floquet branch for the case of time-delayed feedback control. As a result, the stability domain of the orbit controlled by time-delayed feedback as well as by optimal properties of the delayed feedback controller can be evaluated without an explicit integration of time-delay equations. The proposed algorithm gives a better insight into how the Floquet spectrum of periodic orbits controlled by time-delayed feedback is formed. We believe that the ideas of this approach will be useful for further development of the time-delayed feedback control techniques and will stimulate a search for other modifications of the method in order to gain better performance.

In §3, we discussed the main limitation of the DFC method, which states that the method cannot stabilize torsion-free periodic orbits, or more precisely, orbits with an odd number of real-positive Floquet exponents. We have shown that, this topological limitation can be eliminated by introduction into a feedback loop an unstable degree of freedom that changes the total number of unstable torsion-free modes to an even number. An efficiency of the modified scheme has been demonstrated for the Lorenz system.

Lastly, we note that, despite certain progress in the DFC theory, there are still some open problems. Almost all theoretical investigations are based on a linear approach and do not consider an important problem concerning the domain of attraction for target UPOs. The only exception is the recent paper by Yamasue & Hikihara (2004), in which such a domain has been numerically analysed for a Duffing system. We believe that this problem can be considered analytically as well. Recently, we have demonstrated (Pyragas 2004*b*) an analytical treatment for a dynamical system under DFC when the system is close to a subcritical Hopf bifurcation. The analysis has been performed by using the method of averaging, a standard asymptotic method of nonlinear dynamics. In our opinion, an asymptotic method is a promising analytical approach for a nonlinear analysis of delayed feedback-controlled dynamical system close to any bifurcation point of periodic orbit. From this approach, we expect interesting and important theoretical results in the future.

References

Baba, N., Amann, A., Scholl, E. & Just, W. 2002 Giant improvement of time-delayed feedback control by spatio-temporal filtering. *Phys. Rev. Lett.* **89**, 074 101. (doi:10.1103/PhysRevLett.89.074101)

Basso, M., Genesio, R. & Tesi, A. 1997*a* Stabilizing periodic orbits of forced systems via generalized Pyragas controllers. *IEEE Trans. Circuits Syst. I* **44**, 1023–1027. (doi:10.1109/81.633895)

Basso, M., Genesio, R. & Tesi, A. 1997*b* Controller design for extending periodic dynamics of a chaotic CO_2 laser. *Syst. Control Lett.* **31**, 287–297. (doi:10.1016/S0167-6911(97)00044-3)

Basso, M., Genesio, R., Giovanardi, L., Tesi, A. & Torrini, G. 1998 On optimal stabilization of periodic orbits via time delayed feedback control. *Int. J. Bifurc. Chaos Appl. Sci. Eng.* **8**, 1699–1706. (doi:10.1142/S0218127498001376)

Batlle, C., Fossas, E. & Olivar, G. 1999 Stabilization of periodic orbits of the buck converter by time-delayed feedback. *Int. J. Circuit Theory Appl.* **27**, 617–631. (doi:10.1002/(SICI)1097-007X(199911/12)27:6<617::AID-CTA87>3.0.CO;2-R)

Benettin, G., Froeschle, C. & Scheidecker, J. P. 1979 Kolmogorov entropy of a dynamical system with an increasing number of degrees of freedom. *Phys. Rev. A* **19**, 2454–2460. (doi:10.1103/PhysRevA.19.2454)

Benner, H. & Just, W. 2002 Control of chaos by time-delayed feedback in high-power ferromagnetic resonance experiments. *J. Korean Phys. Soc.* **40**, 1046–1050.

Bielawski, S., Derozier, D. & Glorieux, P. 1993 Experimental charakterization of unstable periodic orbits by controlling chaos. *Phys. Rev. A* **47**, R2492–R2495. (doi:10.1103/PhysRevA.47.R2492)

Bielawski, S., Derozier, D. & Glorieux, P. 1994 Controlling unstable periodic orbits by a delayed continuous feedback. *Phys. Rev. E* **49**, R971–R974. (doi:10.1103/PhysRevE.49.R971)

Bleich, M. E. & Socolar, J. E. S. 1996 Stability of periodic orbits controlled by time-delay feedback. *Phys. Lett.* **210A**, 87–94.

Bleich, M. E. & Socolar, J. E. S. 2000 Delayed feedback control of a paced excitable oscillator. *Int. J. Bifurc. Chaos Appl. Sci. Eng.* **10**, 603–609. (doi:10.1142/S0218127400000414)

Bleich, M. E., Hochheiser, D., Moloney, J. V. & Socolar, J. E. S. 1997 Controlling extended systems with spatially filtered, time-delayed feedback. *Phys. Rev. E* **55**, 2119–2126. (doi:10.1103/PhysRevE.55.2119)

Boccaletti, S. & Arecchi, F. T. 1995 Adaptive control of chaos. *Europhys. Lett.* **31**, 127–132.

Boccaletti, S., Farini, A. & Arecchi, F. T. 1997 Adaptive strategies for recognition, control and synchronization of chaos. *Chaos Soliton. Fract.* **8**, 1431–1448. (doi:10.1016/S0960-0779(96)00169-5)

Boccaletti, S., Grebogi, C., Lai, Y.-C., Mancini, H. & Maza, D. 2000 The control of chaos: theory and applications. *Phys. Rep.* **329**, 103–197. (doi:10.1016/S0370-1573(99)00096-4)

Celka, P. 1994 Experimental verification of Pyragas's chaos control method applied to Chua's circuit. *Int. J. Bifurc. Chaos Appl. Sci. Eng.* **4**, 1703–1706. (doi:10.1142/S0218127494001313)

Chen, G. & Raton, B. (eds) 2000. *Controlling chaos and bifurcation in engineering systems*. West Palm Beach, FL: CRS Press.

Chen, G. & Yu, X. (eds) 2003 *Chaos control. Theory and applications*. Berlin, Germany: Springer.

Christini, D. J., In, V., Spano, M. L., Ditto, W. L. & Collins, J. J. 1997 Real-time experimental control of a system in its chaotic and nonchaotic regimes. *Phys. Rev. E* **56**, R3749–R3752. (doi:10.1103/PhysRevE.56.R3749)

Fronczak, P. & Holyst, J. A. 2002 Control of chaotic solitons by a time-delayed feedback mechanism. *Phys. Rev. E* **65**, 026 219. (doi:10.1103/PhysRevE.65.026219)

Fukuyama, T., Shirahama, H. & Kawai, Y. 2002 Dynamical control of the chaotic state of the current-driven ion acoustic instability in a laboratory plasma using delayed feedback. *Phys. Plasmas* **9**, 4525–4529. (doi:10.1063/1.1513469)

Galvanetto, U. 2002 Delayed feedback control of chaotic systems with dry friction. *Int. J. Bifurc. Chaos Appl. Sci. Eng.* **12**, 1877–1883. (doi:10.1142/S0218127402005546)

Gauthier, D. J., Sukow, D. W., Concannon, H. M. & Socolar, J. E. S. 1994 Stabilizing unstable periodic orbits in a fast diode resonator using continous time-delay autosynchronization. *Phys. Rev. E* **50**, 2343–2346. (doi:10.1103/PhysRevE.50.2343)

Gravier, E., Caron, X., Bonhomme, G., Pierre, T. & Briancon, J. L. 2000 Dynamical study and control of drift waves in a magnetized laboratory plasma. *Eur. J. Phys.* **8D**, 451–456.

Guderian, A., Munster, A. F., Kraus, M. & Schneider, F. W. 1998 Electrochemical chaos control in a chemical reaction: experiment and simulation. *J. Phys. Chem. A* **102**, 5059–5064. (doi:10.1021/jp980997g)

Hall, K., Christini, D. J., Tremblay, M., Collins, J. J., Glass, L. & Billette, J. 1997 Dynamic control of cardiac alternans. *Phys. Rev. Lett.* **78**, 4518–4521. (doi:10.1103/PhysRevLett.78.4518)

Herrmann, G. 2001 A robust delay adaptation scheme for Pyragas' chaos control method. *Phys. Lett.* **287A**, 245–256.

Hikihara, T. & Kawagoshi, T. 1996 Experimental study on stabilization of unstable periodic motion in magneto-elastic chaos. *Phys. Lett.* **211A**, 29–36.

Hochheiser, D., Moloney, J. V. & Lega, J. 1997 Controlling optical turbulence. *Phys. Rev. A* **55**, R4011–R4014. (doi:10.1103/PhysRevA.55.R4011)

Holyst, J. A. & Urbanowicz, K. 2000 Chaos control in economical model by time-delayed feedback method. *Physica* **287A**, 587–598.

Holyst, J. A., Zebrowska, M. & Urbanowicz, K. 2001 Observations of deterministic chaos in financial time series by recurrence plots, can one control chaotic economy? *Eur. Phys. J.* **20B**, 531–535.

Just, W., Bernard, T., Ostheimer, M., Reibold, E. & Benner, H. 1997 Mechanism of time-delayed feedback control. *Phys. Rev. Lett.* **78**, 203–206. (doi:10.1103/PhysRevLett.78.203)

Just, W., Reibold, E., Benner, H., Kacperski, K., Fronczak, P. & Holyst, J. 1999 Limits of time-delayed feedback control. *Phys. Lett.* **254A**, 158–164.

Just, W., Reibold, E., Kacperski, K., Fronczak, P., Holyst, J. A. & Benner, H. 2000 Influence of stable Floquet exponents on time-delayed feedback control. *Phys. Rev. E* **61**, 5045–5056. (doi:10.1103/PhysRevE.61.5045)

Kapitaniak, T. 1996 *Controlling chaos. Theoretical and practical methods in non-linear dynamics.* London, UK: Academic Press.

Kittel, A., Parisi, J., Pyragas, K. & Richter, R. 1994 Delayed feedback control of chaos in an electronic double-scroll oscillator. *Z. Naturforsch.* **49A**, 843–846.

Kittel, A., Parisi, J. & Pyragas, K. 1995 Delayed feedback control of chaos by self-adapted delay time. *Phys. Lett.* **198A**, 433–438.

Konishi, K., Kokame, H. & Hirata, H. K. 1999 Coupled map car-following model and its delayed-feedback control. *Phys. Rev. E* **60**, 4000–4007. (doi:10.1103/PhysRevE.60.4000)

Krodkiewski, J. M. & Faragher, J. S. 2000 Stabilization of motion of helicopter rotor blades using delayed feedback–modelling, computer simulation and experimental verification. *J. Sound Vib.* **234**, 591–610. (doi:10.1006/jsvi.1999.2878)

Lathrop, D. P. & Kostelich, E. J. 1989 Characterization of an experimental strange attractor by periodic orbits. *Phys. Rev. A* **40**, 4028–4031. (doi:10.1103/PhysRevA.40.4028)

Lorenz, E. N. 1963 Deterministic non-periodic flow. *J. Atmos. Sci.* **20**, 130–141. (doi:10.1175/1520-0469(1963)020<0130:DNF>2.0.CO;2)

Lu, W., Yu, D. & Harrison, R. G. 1998 Instabilities and tracking of travelling wave patterns in a three-level laser. *Int. J. Bifurc. Chaos Appl. Sci. Eng.* **8**, 1769–1775. (doi:10.1142/S0218127498001479)

Lüthje, O., Wolff, S. & Pfister, G. 2001 Control of chaotic Taylor-Couette flow with time-delayed feedback. *Phys. Rev. Lett.* **86**, 1745–1748.

Mausbach, Th., Klinger, Th., Piel, A., Atipo, A. & Pierre, Th. 1997 Continuous control of ionization wave chaos by spatially derived feedback signals. *Phys. Lett.* **228A**, 373–377.

Mensour, B. & Longtin, A. 1995 Controlling chaos to store information in delay-differential equations. *Phys. Lett.* **205A**, 18–24.

Mitsubori, K. & Aihara, K. U. 2002 Delayed-feedback control of chaotic roll motion of a flooded ship in waves. *Proc. R. Soc. A* **458**, 2801–2813. (doi:10.1098/rspa.2002.1012)

Munkel, M., Kaiser, F. & Hess, O. 1997 Stabilization of spatiotemporally chaotic semiconductor laser arrays by means of delayed optical feedback. *Phys. Rev. E* **56**, 3868–3875.

Nakajima, H. 1997 On analytical properties of delayed feedback control of chaos. *Phys. Lett.* **232A**, 207–210.

Nakajima, H. & Ueda, Y. 1998*a* Limitation of generalized delayed feedback control. *Physica* **111D**, 143–150.

Nakajima, H. & Ueda, Y. 1998*b* Half-period delayed feedback control for dynamical systems with symmetries. *Phys. Rev. E* **58**, 1757–1763. (doi:10.1103/PhysRevE.58.1757)

Nakajima, H., Ito, H. & Ueda, Y. 1997 Automatic adjustment of delay time acid feedback gain in delayed feedback control of chaos. *IEICE Trans. Fundam. Electron. Commun. Comput. Sci.* **E80A**, 1554–1559.

Ott, E., Grebogi, C. & Yorke, J. A. 1990 Controlling chaos. *Phys. Rev. Lett.* **64**, 1196–1199. (doi:10.1103/PhysRevLett.64.1196)

Parmananda, P., Madrigal, R., Rivera, M., Nyikos, L., Kiss, I. Z. & Gaspar, V. 1999 Stabilization of unstable steady states and periodic orbits in an electrochemical system using delayed-feedback control. *Phys. Rev. E* **59**, 5266–5271. (doi:10.1103/PhysRevE.59.5266)

Pierre, T., Bonhomme, G. & Atipo, A. 1996 Controlling the chaotic regime of nonlinear ionization waves using the time-delay autosynchronization method. *Phys. Rev. Lett.* **76**, 2290–2293. (doi:10.1103/PhysRevLett.76.2290)

Pyragas, K. 1992 Continuous control of chaos by self-controlling feedback. *Phys. Lett.* **170A**, 421–428.

Pyragas, K. 1995 Control of chaos via extended delay feedback. *Phys. Lett.* **206A**, 323–330.

Pyragas, K. 2001 Control of chaos via an unstable delayed feedback controller. *Phys. Rev. Lett.* **86**, 2265–2268. (doi:10.1103/PhysRevLett.86.2265)

Pyragas, K. 2002 Analytical properties and optimization of time-delayed feedback control. *Phys. Rev. E* **66**, 026207. (doi:10.1103/PhysRevE.66.026207)

Pyragas, K. & Tamaševičius, A. 1993 Experimental control of chaos by delayed self-controlling feedback. *Phys. Lett.* **180A**, 99–102.

Pyragas, K., Pyragas, V., Kiss, I. Z. & Hudson, J. L. 2002 Stabilizing and tracking unknown steady states of dynamical systems. *Phys. Rev. Lett.* **89**, 244 103. (doi:10.1103/PhysRevLett.89.244103)

Pyragas, K., Pyragas, V., Kiss, I. Z. & Hudson, J. L. 2004*a* Adaptive control of unknown unstable steady states of dynamical systems. *Phys. Rev. E* **70**, 026 215. (doi:10.1103/PhysRevE.70.026215)

Pyragas, K., Pyragas, V. & Benner, H. 2004*b* Delayed feedback control of dynamical systems at a subcritical Hopf bifurcation. *Phys. Rev. E* **70**, 056 222. (doi:10.1103/PhysRevE.70.056222)

Rappel, W. J., Fenton, F. & Karma, A. 1999 Spatiotemporal control of wave instabilities in cardiac tissue. *Phys. Rev. Lett.* **83**, 456–459. (doi:10.1103/PhysRevLett.83.456)

Rosenblum, M. & Pikovsky, A. 2004*a* Controlling synchronization in an ensemble of globally coupled oscillators. *Phys. Rev. Lett.* **92**, 114 102. (doi:10.1103/PhysRevLett.92.114102)

Rosenblum, M. & Pikovsky, A. 2004*b* Delayed feedback control of collective synchrony: an approach to suppression of pathological brain rhythms. *Phys. Rev. E* **70**, 041 904. (doi:10.1103/PhysRevE.70.041904)

Rössler, O. E. 1976 An equation for continous chaos. *Phys. Lett.* **57A**, 397–398.

Shinbrot, T., Grebogy, C., Ott, E. & Yorke, J. A. 1993 Using small perturbations to control chaos. *Nature* **363**, 411–417. (doi:10.1038/363411a0)

Shuster, H. G. (ed.) 1999. *Handbook of chaos control*. Weinheim, Germany: Wiley/VCH.

Simmendinger, C. & Hess, O. 1996 Controlling delay-induced chaotic behavior of a semiconductor laser with optical feedback. *Phys. Lett.* **21A**, 97–105.

Simmendinger, C., Munkel, M. & Hess, O. 1999 Controlling complex temporal and spatio-temporal dynamics in semiconductor lasers. *Chaos Soliton. Fract.* **10**, 851–864. (doi:10.1016/S0960-0779(98)00037-X)

So, P., Ott, E., Schiff, S. J., Kaplan, D. T., Sauer, T. & Grebogi, C. 1996 Detecting unstable periodic orbits in chaotic experimental data. *Phys. Rev. Lett.* **76**, 4705–4708. (doi:10.1103/PhysRevLett.76.4705)

Socolar, J. E. S., Sukow, D. W. & Gauthier, D. J. 1994 Stabilizing unstable periodic orbits in fast dynamical systems. *Phys. Rev. E* **50**, 3245–3248. (doi:10.1103/PhysRevE.50.3245)

Sugimoto, Y. & Osuka, K. 2002 Walking control of quasi-passive-dynamic-walking robot "Quartet III" based on delayed feedback control. In *Proceedings of the 5th International Conference on Climbing and Walking Robots(CLAWAR)*, pp. 123–130.

Tsui, A. P. M. & Jones, A. J. 2000 The control of higher dimensional chaos: comparative results for the chaotic satellite attitude control problem. *Physica* **135D**, 41–62.

Ushio, T. 1996 Limitation of delayed feedback control in nonlinear discrete-time systems. *IEEE Trans. Circuits Syst. I* **43**, 815–816. (doi:10.1109/81.536757)

Yamasue, K. & Hikihara, T. 2004 Domain of attraction for stabilized orbits in time delayed feedback controlled Duffing systems. *Phys. Rev. E* **69**, 056 209. (doi:10.1103/PhysRevE.69.056209)